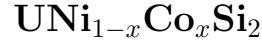


On the search for quantum criticality in a ferromagnetic system



A. P. Pikul and D. Kaczorowski

Institute of Low Temperature and Structure Research,

Polish Academy of Sciences, P Nr 1410, 50–590 Wrocław 2, Poland

(Dated: November 11, 2018)

Abstract

Polycrystalline samples of the isostructural alloys $\text{UNi}_{1-x}\text{Co}_x\text{Si}_2$ ($0 \leq x \leq 1$) were studied by means of x-ray powder diffraction, magnetization, electrical resistivity and specific heat measurements, at temperatures down to 2 K and in magnetic fields up to 5 T. The experimental data revealed an evolution from strongly anisotropic ferromagnetism with pronounced Kondo effect, observed for the alloys with $x < 0.98$ and being gradually suppressed with rising Co-content, to spin-glass-like states with dominant spin fluctuations, seen for the sample with $x = 0.98$. Extrapolation of the value of $T_C(x)$ yields a critical concentration $x_c = 1$, at which the magnetic ordering entirely disappears. This finding is in line with preliminary data collected for stoichiometric UCoSi_2 .

PACS numbers: 75.40.-s; 71.27.+a

I. INTRODUCTION

Since a few years the unusual physical behaviors of f -electron systems being at the verge of magnetic ordering have been at the very forefront of modern condensed matter physics [1–5]. The so-called quantum phase transition (QPT) occurs at the absolute zero temperature and is driven by quantum fluctuations, instead of thermal fluctuations associated with phase transitions at finite temperatures. If such a transition has a continuous (2nd order) character one speaks about a quantum critical point (QCP).

Most of the hitherto performed experimental studies on the quantum criticality (independently of the theoretical scenarios considered) were devoted to numerous non-stoichiometric alloys and stoichiometric compounds based on cerium, ytterbium or uranium, which exhibit antiferromagnetic correlations [1,2]. Ferromagnetic quantum phase transitions are much less known both from the theoretical and experimental point of views [1,2,6]. Therefore, it is particularly tempting to investigate systems in which ferromagnetism can be tuned down to the absolute zero temperature by external parameters, like pressure, magnetic field or/and composition. Amidst very rare examples of alloys, in which ferromagnetism gets suppressed (or induced) by chemical doping, one can mention i.a. $U_xTh_{1-x}Cu_2Si_2$ [7], Ni_xPd_{1-x} [8], $CePd_{1-x}Ni_x$ [9], $CePd_{1-x}Rh_x$ [10–12], $URu_{2-x}Re_xSi_2$ [13], $URh_{1-x}Ru_xGe$ [14] and $UCoGe_{1-x}Si_x$ [15]. The number of stoichiometric compounds for which the presence of pressure-induced ferromagnetic QPT has been demonstrated is extremely small, with the most prominent examples being UGe_2 [16], $URhGe$ [17], $UCoGe$ [18]. Remarkably, up to date the only stoichiometric ferromagnet claimed to exhibit a second-order quantum phase transition seems $CePt$ [19].

The ternary uranium silicides $UTSi_2$ ($T = Fe, Co, Ni$), crystallizing with the orthorhombic $CeNiSi_2$ -type crystal structure, were reported to span a variety of magnetic properties driven by the hybridization between U $5f$ - and T $3d$ -electronic states. Whereas $UNiSi_2$ is a ferromagnetically ordered ($T_C = 95$ K) Kondo lattice with relatively well localized $5f$ -electrons [20–22], $UCoSi_2$ behaves as a spin fluctuation system, and $UFe_{1-y}Si_2$ shows features of a weakly temperature dependent Pauli paramagnet [20]. The previous findings motivated us to undertake a detailed study on the solid solution $UNi_{1-x}Co_xSi_2$ ($0 \leq x \leq 1$), with the main focus on the alloys being close to a ferromagnetic instability, expected to occur for a certain Co-content x_c . Our first attempt was to check for a possible non-Fermi-liquid

character of the dc magnetic susceptibility, electrical resistivity and heat capacity of the specimens having nearly critical composition. The aim of this paper is to show that the ferromagnetic behavior in $\text{UNi}_{1-x}\text{Co}_x\text{Si}_2$ is observed in a nearly complete solution range and that the critical concentration x_c is fairly close to 1. In other words, our experimental data point at possible ferromagnetic quantum critical behavior in stoichiometric UCoSi_2 .

II. EXPERIMENTAL DETAILS

Polycrystalline samples of the solid solutions $\text{UNi}_{1-x}\text{Co}_x\text{Si}_2$ ($0 \leq x \leq 1$) were synthesized by conventional arc melting the nominal amounts of the constituents under protective atmosphere of an argon glove box. The pellets were subsequently wrapped in a tantalum foil, sealed in evacuated silica tubes, and annealed at 800°C for 2 weeks. Quality of the products was verified by means of x-ray powder diffraction measurements (X'pert Pro PANalytical diffractometer with Cu $K\alpha$ radiation; $\lambda = 1.54056 \text{ \AA}$). Magnetic properties were studied at temperatures ranging from 1.7 up to room temperature and in applied magnetic fields up to 5 T, using a Quantum Design SQUID (superconducting quantum interference device) magnetometer and a Cryogenics AC susceptometer. The electrical resistivity was measured down to 4.2 K in zero magnetic field using a standard DC four-point probe method implemented in a home-made setup, on bar-shaped specimens with spot-welded electrical contacts. Heat capacity studies were carried out at temperatures 2 K – 300 K and in applied magnetic fields up to 9 T employing a thermal relaxation technique implemented in a Quantum Design PPMS (Physical Property Measurement System).

III. RESULTS AND DISCUSSION

A. Crystal structure

Analysis of the experimental x-ray powder diffraction patterns obtained for the alloys $\text{UNi}_{1-x}\text{Co}_x\text{Si}_2$ (not shown here) revealed that all the specimens used in the present study were nearly single phases with very small amount (less than 5%) of same unidentified impurity phase. Rietveld refinements confirmed that the entire system crystallizes with the orthorhombic ($Cmmm$) CeNiSi_2 -type structure [Fig. 1(a)]. The lattice parameters derived for UNiSi_2 ($a = 4.006 \text{ \AA}$, $b = 16.070 \text{ \AA}$ and $c = 4.002 \text{ \AA}$) are in good agreement with the

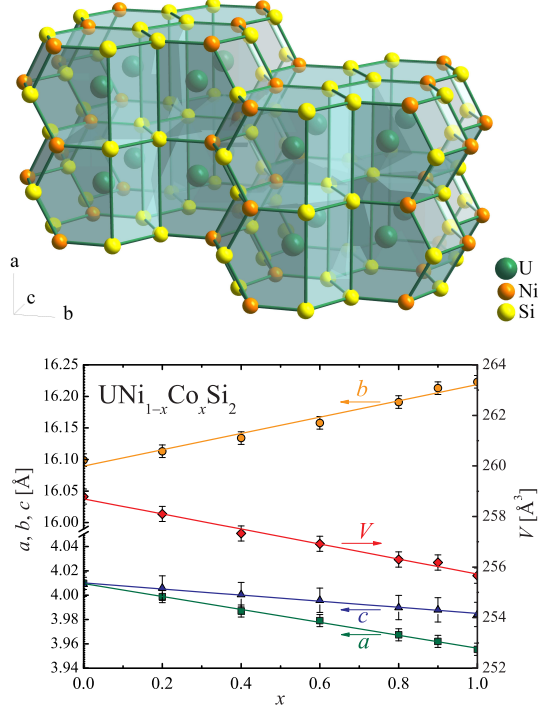


FIG. 1: (Color online) (a) Crystal structure of UNiSi₂. (b) Lattice parameters and unit cell volume of the solid solutions UNi_{1-x}Co_xSi₂ as a function of the Co content x .

literature data [20]. As can be inferred from Fig. 1(b), the isostructural, partial substitution of Ni atoms by about 0.8% larger Co atoms expands linearly the unit cell along the b axis (in total by +0.8%) yet reduces it along the a and c axes (in total by -1.4% and -0.6%, respectively), leading eventually to the contraction in the unit cell volume of the system by about -1.2%. The lattice parameters of the terminal compound UCoSi₂ were found to be equal to $a = 3.956$ Å, $b = 16.223$ Å and $c = 3.984$ Å, being close to those reported previously [20].

B. Magnetic properties

Figure 2(a) presents the inverse molar magnetic susceptibility χ^{-1} of the alloys UNi_{1-x}Co_xSi₂ ($0 \leq x \leq 1$) as a function of temperature T . As seen, above about 150 K all the experimental curves exhibit quasi-linear behavior that can be described by the modified Curie–Weiss law:

$$\chi(T) = \frac{1}{8} \frac{\mu_{\text{eff}}^2}{T - \theta_p} + \chi_0, \quad (1)$$

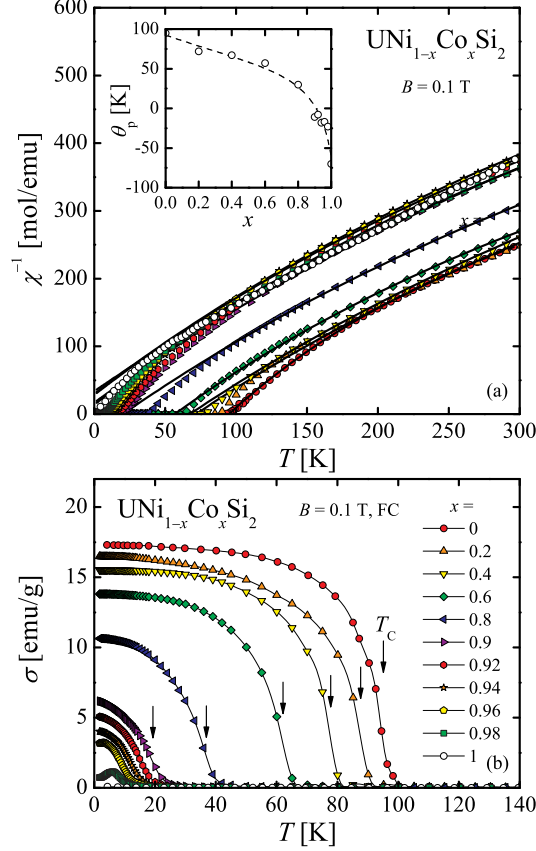


FIG. 2: (Color online) (a) Temperature dependencies of the inverse molar magnetic susceptibility of the alloys $\text{UNi}_{1-x}\text{Co}_x\text{Si}_2$ measured in magnetic field $B = 0.1$ T. Solid lines are fits of the modified Curie–Weiss law (Eq. (1)) to the experimental data. The inset displays the Weiss temperature θ_p as a function of x ; the dashed line serves as a guide for the eye. (b) Temperature variations of the magnetization of $\text{UNi}_{1-x}\text{Co}_x\text{Si}_2$ measured in $B = 0.1$ T in a field-cooling (FC) regime. Thin solid lines serve as guides for the eye; the arrows mark the ordering temperatures T_C .

where μ_{eff} is the effective magnetic moment, θ_p is the paramagnetic Weiss temperature, and χ_0 is a temperature independent term accounting for Pauli paramagnetism of the conduction electrons and diamagnetism of the core electrons. Least squares fits of Eq. (1) to the experimental data [see the solid lines in Fig. 2(a)] yielded for each $\text{UNi}_{1-x}\text{Co}_x\text{Si}_2$ compound a value of $\mu_{\text{eff}} \sim 2.3 \mu_B$ and $\chi_0 \sim 8 \times 10^{-4}$ emu/mol. In turn, θ_p was found to decrease monotonically from 95 K in UNiSi_2 to -70 K in UCoSi_2 [see the inset to Fig. 2(a)]. The experimental value of μ_{eff} is moderately reduced in comparison to the theoretical one, calculated for free U^{3+} ($3.62 \mu_B$) or U^{4+} ($3.58 \mu_B$) ions, and χ_0 is somewhat larger than usually observed in conventional metals. It suggests that the uranium $5f$ electrons in $\text{UNi}_{1-x}\text{Co}_x\text{Si}_2$

are partly delocalized, as commonly observed in U-based intermetallics. Because μ_{eff} and χ_0 hardly changes upon increasing x one can conclude, that the degree of delocalization of the $5f$ electrons in this system remains unaffected by the Ni/Co substitution. In turn, the decreasing positive θ_p can be ascribed to weakening of an inter-site ferromagnetic coupling between the uranium magnetic moments. For large x it becomes obscured by a negative contribution most likely due to strong electronic correlations or an inter-site antiferromagnetic coupling.

Figure 2(b) displays the temperature dependencies of the magnetization σ of $\text{UNi}_{1-x}\text{Co}_x\text{Si}_2$. The characteristic Brillouin-shaped anomalies on $\sigma(T)$ indicate the ferromagnetic ordering in the alloys with $x \leq 0.96$. Upon increasing the Co content, the Curie temperature T_C decreases from 95 K in UNiSi_2 (in agreement with the literature data [20]) down to 8.6 K in $\text{UNi}_{0.04}\text{Co}_{0.96}\text{Si}_2$. Simultaneously, the magnitude of the magnetization notably decreases. Eventually, for $x > 0.96$, the ferromagnetic anomaly evolves into a broad maximum of unclear origin, while in pure UCoSi_2 no anomaly in $\sigma(T)$ is observed down to 1.7 K.

The results of detailed investigations of the magnetic properties of two representative compositions from the range $x \leq 0.96$, namely UNiSi_2 and $\text{UNi}_{0.4}\text{Co}_{0.6}\text{Si}_2$, are displayed in Figs. 3 and 4, respectively. For both compounds $\sigma(T)$ measured in zero-field-cooled and field-cooled regimes shows a pronounced bifurcation below the Curie temperature, characteristic of strongly anisotropic ferromagnets with pronounced domain effects. The negative values of the ZFC magnetization result most likely from the presence of remnant magnetic field, hardly avoidable in experiments performed using standard superconducting magnets. The overall shape of the isothermal field dependence of the magnetization measured deeply in the ordered state [see the insets to Figs. 3 and 4] provides another strong evidence for the ferromagnetic ground state in UNiSi_2 and $\text{UNi}_{0.4}\text{Co}_{0.6}\text{Si}_2$. In particular, in low magnetic fields the magnetization rapidly increases with B and saturates at high fields, reaching at $B = 5$ T a value corresponding to about $1.2 \mu_B$ (UNiSi_2) and $0.9 \mu_B$ ($\text{UNi}_{0.4}\text{Co}_{0.6}\text{Si}_2$). Remarkably, the two $\sigma(B)$ curves exhibit strongly hysteretic behavior and very high remanence of about 19 (for $x = 0.0$) and 13.5 emu/g (for $x = 0.6$), both features being characteristic of hard ferromagnets. The magnetic properties of the other alloys $\text{UNi}_{1-x}\text{Co}_x\text{Si}_2$ from the range $x \leq 0.96$ are qualitatively very similar to those of UNiSi_2 and $\text{UNi}_{0.4}\text{Co}_{0.6}\text{Si}_2$, yet the hysteresis and the saturated moment both gradually diminish with increasing x .

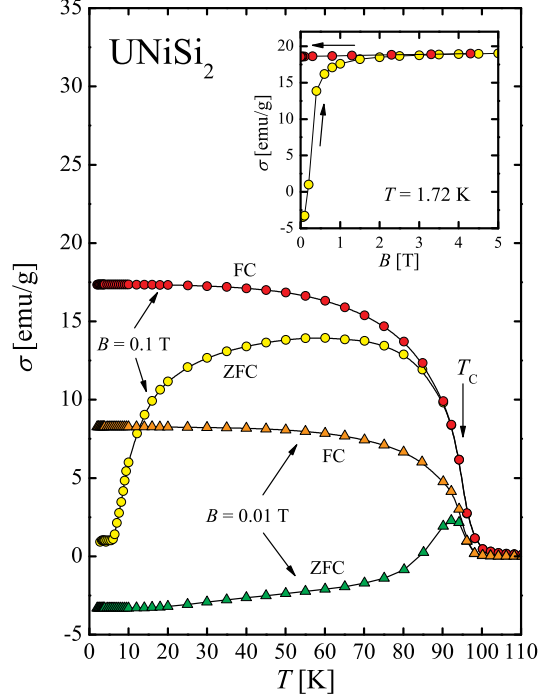


FIG. 3: (Color online) Temperature variations of the magnetization σ of UNiSi_2 measured in two different magnetic fields B in the zero-field-cooling (ZFC) and the field-cooling (FC) regime. The solid lines serve as guides for the eye; T_C marks the Curie temperature. The inset: σ measured at constant temperature $T = 1.72$ K as a function of increasing (open symbols) and decreasing (closed symbols) magnetic field B .

Figure 5 presents the magnetic properties of $\text{UNi}_{0.02}\text{Co}_{0.98}\text{Si}_2$. Apparently, the overall shape of the FC $\sigma(T)$ curve measured for this composition is much different from that observed for the ferromagnetically ordered alloys (i.e. with $x \leq 0.96$). In particular, the Brillouin-like curvature is not seen, and instead the $\sigma(T)$ curve forms a broad maximum at about 6 K. Moreover, the magnitude of the magnetization of $\text{UNi}_{0.02}\text{Co}_{0.98}\text{Si}_2$ is almost 20 times smaller than the value measured for the parent compound UNiSi_2 [Fig. 3], the hysteresis in $\sigma(B)$ [see the inset to Fig. 5] is hardly visible, and σ does not saturate in high fields. All these features indicate a change in the character of the magnetic ordering from the long-range ferromagnetic one for $x \leq 0.96$ to a spin-glass-like state for $x = 0.98$, probably governed by an interplay of competing ferromagnetic and antiferromagnetic interactions.

In agreement with the previous report [20], the terminal alloy UCoSi_2 is a Curie-Weiss paramagnet down to the lowest temperature studied (cf. Fig. 2). Accordingly, its mag-

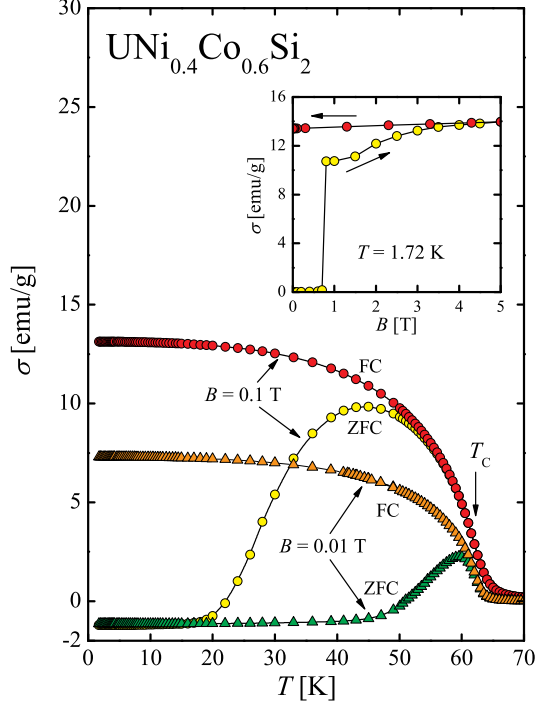


FIG. 4: (Color online) Temperature variations of the magnetization σ of $\text{UNi}_{0.4}\text{Co}_{0.6}\text{Si}_2$ measured in two different magnetic fields B in the zero-field-cooling (ZFC) and the field-cooling (FC) regime. The solid lines serve as guides for the eye; T_C marks the Curie temperature. The inset: σ measured at constant temperature $T = 1.72$ K as a function of increasing (open symbols) and decreasing (closed symbols) magnetic field B .

netization does not exhibit any hysteresis effect neither in the field nor the temperature dependence (not shown here).

C. Electrical resistivity

Temperature dependencies of the electrical resistivity ρ of the $\text{UNi}_{1-x}\text{Co}_x\text{Si}_2$ alloys are plotted in Fig. 6. In the paramagnetic region, the electrical resistivity of the alloys with $x \leq 0.60$ increases with decreasing temperature. Upon further substitution of Ni atoms by Co atoms, the $\rho(T)$ curve changes its slope into a positive one in the entire temperature range studied.

At low temperatures, pronounced drops of the resistivity manifest the ferromagnetic phase transitions in the alloys with $x \leq 0.94$. Positions of the anomalies in $\rho(T)$, defined as inflec-

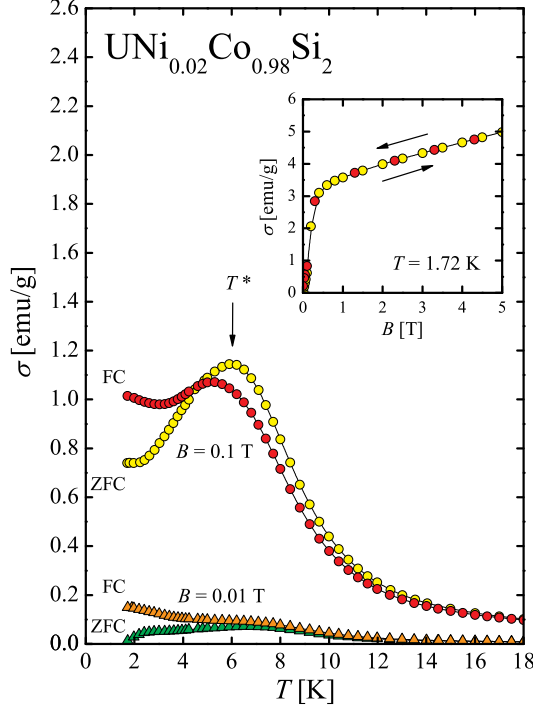


FIG. 5: (Color online) Temperature variations of the magnetization σ of $\text{UNi}_{0.02}\text{Co}_{0.98}\text{Si}_2$ measured in two different magnetic fields B in the zero-field-cooling (ZFC) and the field-cooling (FC) regime. The solid lines serve as guides for the eye and the arrows mark the phase transition temperatures. The inset: σ measured at constant temperature $T = 1.72$ K as a function of increasing (open symbols) and decreasing (closed symbols) magnetic field B .

tion points in $d\rho(T)/dT$ (cf. Fig. 7), correspond to the Curie temperatures estimated from the magnetization data [cf. Fig. 2(b)]. For the Co-rich alloys $\text{UNi}_{0.04}\text{Co}_{0.96}\text{Si}_2$ ($T_C = 8.6$ K) and $\text{UNi}_{0.02}\text{Co}_{0.98}\text{Si}_2$ ($T^* = 6$ K), the phase transitions are hardly visible in the resistivity data.

The increase of the resistivity with decreasing T , that is observed for $x \leq 0.60$ in the paramagnetic region, may result from the spin-flip Kondo scattering the conduction electrons on magnetic moments of the uranium atoms. Indeed, the experimental data can be described above T_C by the formula [20]:

$$\rho(T) = (\rho_0 + \rho_0^\infty) - c_K \log T, \quad (2)$$

where the first term stands for temperature independent scattering the conduction electrons on static defects and disordered magnetic moments, and the second one describes the Kondo effect. Solid lines in Fig. 7 display the results of the least-square

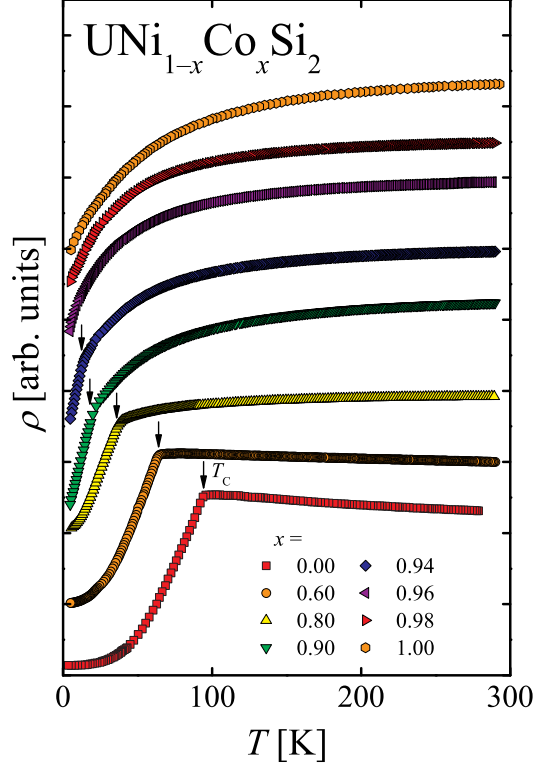


FIG. 6: (Color online) Temperature dependencies of the electrical resistivity ρ of the alloys $\text{UNi}_{1-x}\text{Co}_x\text{Si}_2$ with selected Co-content; the curves are shifted upwards for clarity. The arrows mark the ordering temperatures T_C and the solid lines emphasize logarithmic temperature dependence of ρ .

fits for UNiSi_2 [$(\rho_0 + \rho_0^\infty) = 319.6(1) \mu\Omega\text{cm}$, $c_K = 52.6(1) \mu\Omega\text{cm}$] and $\text{UNi}_{0.4}\text{Co}_{0.6}\text{Si}_2$ [$(\rho_0 + \rho_0^\infty) = 396.2(1) \mu\Omega\text{cm}$, $c_K = 16.9(1) \mu\Omega\text{cm}$]. The values of the fitting parameters for UNiSi_2 are of the same order as those given in Ref. 20. The observed decrease in the value of c_K on going from UNiSi_2 to $\text{UNi}_{0.4}\text{Co}_{0.6}\text{Si}_2$ manifests suppression of the Kondo effect in the system with increasing x , in line with the observed evolution of $\rho(T)$ towards strongly bent metallic-like dependence found for the Co-rich samples.

In the ordered region, the resistivity of both alloys is dominated by the contributions due to scattering the conduction electrons on ferromagnetic spin waves [20]:

$$\rho(T) = \rho_0 + AT^2 \exp\left(-\frac{\Delta}{T}\right), \quad (3)$$

where ρ_0 is the residual resistivity, Δ is a gap in the spin-waves spectrum, and c_m is a coefficient of proportionality. Fits of Eq. (3) to the experimental data below about $0.8 T_C$ yielded the values $\rho_0 = 13.9 \mu\Omega\text{cm}$, $c_m = 0.06(1) \mu\Omega\text{cm}/\text{K}^2$ and $\Delta = 87(1) \text{K}$ for UNiSi_2 ,

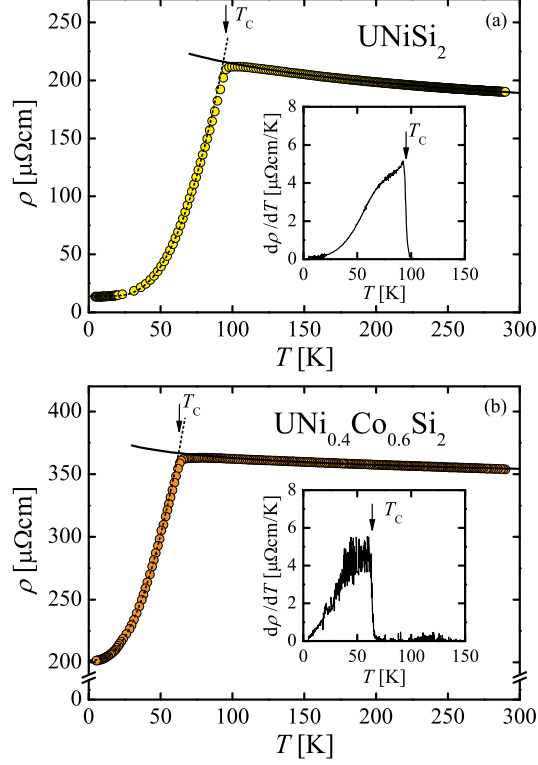


FIG. 7: (Color online) Temperature dependence of the electrical resistivity ρ of (a) UNiSi_2 and (b) $\text{UNi}_{0.4}\text{Co}_{0.6}\text{Si}_2$. The arrows mark the ordering temperatures T_C , the solid and the dashed line show fits of Eqs. (2) and (3), respectively, to the experimental data. The insets show temperature derivatives of the resistivity, $d\rho(T)/dT$; the arrows mark the Curie temperatures T_C .

and $\rho_0 = 201.8 \mu\Omega\text{cm}$, $c_m = 0.05(1) \mu\Omega\text{cm}/\text{K}^2$ and $\Delta = 15(1) \text{ K}$ for $\text{UNi}_{0.4}\text{Co}_{0.6}\text{Si}_2$ (see the dashed lines in Fig. 7). The values obtained for UNiSi_2 somewhat differ from those reported in Ref. 20, most probably due to distinctly different ranges of the data analysis.

Figure 8 presents the temperature dependencies of the electrical resistivity of the Co-rich sample $\text{UNi}_{0.02}\text{Co}_{0.98}\text{Si}_2$ and the terminal compound UCoSi_2 . As seen, the overall shapes of these two $\rho(T)$ curves are reminiscent of metallic systems with strong spin fluctuations, like e.g. Np , Pu , or UAl_2 . Both $\rho(T)$ and the derivative $d\rho(T)/dT$ calculated for UCoSi_2 are featureless down to the lowest temperatures studied. Also for $\text{UNi}_{0.02}\text{Co}_{0.98}\text{Si}_2$ no anomaly in the electrical transport is seen, which could be associated with the feature at T^* revealed in the magnetic susceptibility data (broad and blurred extremum observed in $d\rho(T)/dT$ is likely due to experimental noise).

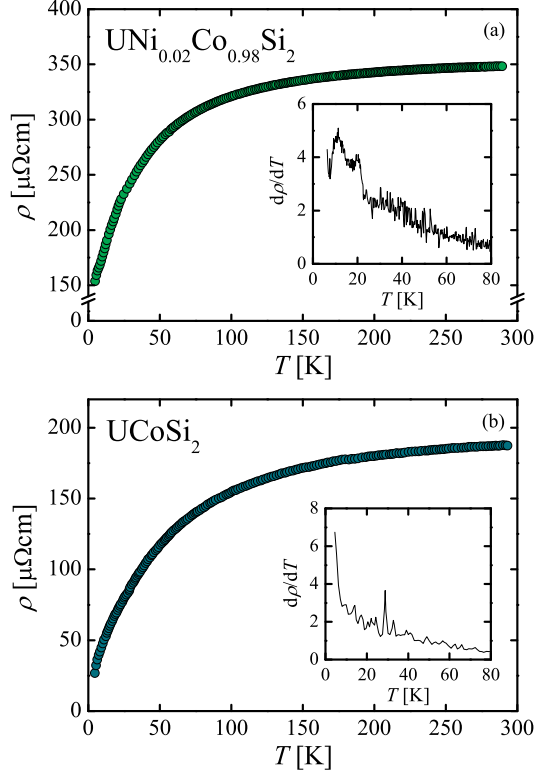


FIG. 8: (Color online) Temperature dependence of the electrical resistivity ρ of (a) $\text{UNi}_{0.02}\text{Co}_{0.98}\text{Si}_2$ and (b) UCoSi_2 . The insets show temperature derivatives $d\rho(T)/dT$.

D. Specific heat

Figure 9(a) presents the temperature variations of the specific heat of selected $\text{UNi}_{1-x}\text{Co}_x\text{Si}_2$ alloys and their isostructural phonon counterpart ThCoSi_2 . Above about 110 K, the heat capacity data obtained for each alloy overlap the $C(T)$ curve of the latter compound, indicating that in this temperature range the possible Schottky contribution due to crystal electric field is negligibly small in comparison to the total specific heat measured. Presence of a distinct λ -shaped peak in $C(T)$ at T_C confirms bulk character of the long-range ferromagnetic ordering in UNiSi_2 . For $\text{UNi}_{0.40}\text{Co}_{0.60}\text{Si}_2$ the magnetic anomaly is still clearly visible, yet it is significantly smaller and somewhat broader. In contrast, in the $C(T)$ data of the Co-richest alloy $\text{UNi}_{0.02}\text{Co}_{0.98}\text{Si}_2$ hardly any singularity is seen. The encountered evolution of the λ -peak is entirely in line with the suppression of the ferromagnetic order in $\text{UNi}_{1-x}\text{Co}_x\text{Si}_2$ observed in the $\sigma(T)$ and $\rho(T)$ characteristics.

Figure 9(b) displays the temperature dependencies of the excess specific heat ΔC due

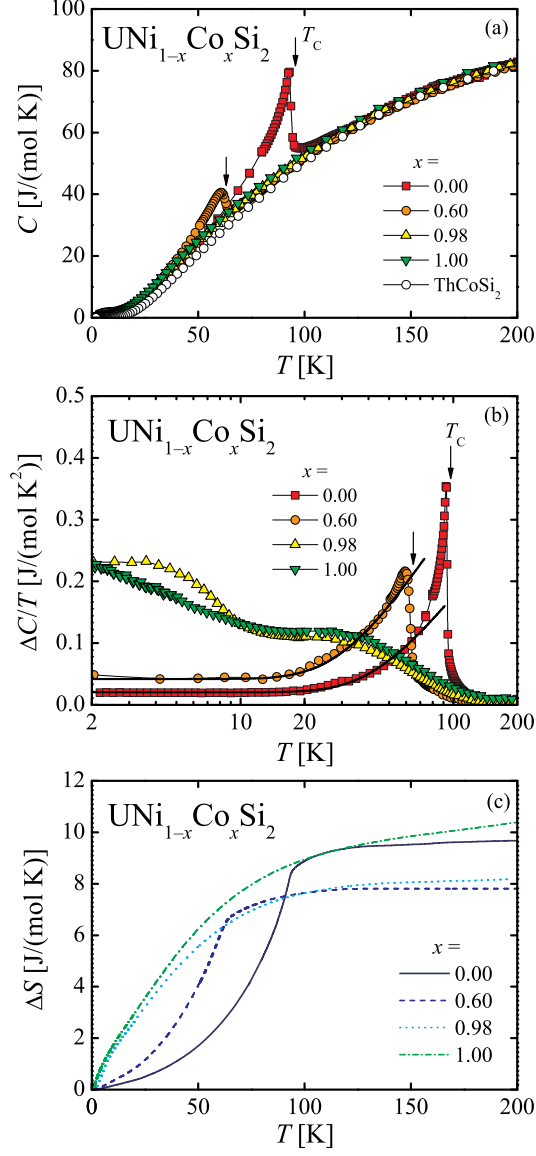


FIG. 9: (Color online) (a) Temperature dependencies of the specific heat C of selected UNi_{1-x}Co_xSi₂ alloys and ThCoSi₂. The arrows mark the ordering temperatures T_C . (b) Magnetic contribution ΔC divided by T in logarithmic scale. Solid lines are fits of Eq. (4) to the experimental data. (c) Temperature dependencies of the excess magnetic entropy ΔS in selected UNi_{1-x}Co_xSi₂ alloys. The arrows mark the ordering temperatures T_C .

to $5f$ -electrons divided by T , obtained for a few UNi_{1-x}Co_xSi₂ subtracting the $C(T)$ data of nonmagnetic ThCoSi₂ from the heat capacity of these alloys. The specific heat of the ferromagnetically ordered compounds can be described below about $0.8T_C$ by the formula

developed for thermally excited ferromagnetic magnons (cf. Ref. 23):

$$\Delta C(T) = \gamma^* T + BT^{3/2} \exp\left(-\frac{\Delta}{T}\right). \quad (4)$$

where γ^* is the Sommerfeld coefficient due to partly delocalized $5f$ -electrons of uranium, Δ stands for the gap in the spin-wave spectrum, and B is a coefficient of proportionality. Least squares fits of Eq. (4) to the experimental data yielded for UNiSi_2 : $\gamma^* = 20(1)$ mJ/(molK²), $B = 36(1)$ mJ/(molK⁴) and $\Delta = 81(1)$ K, and for $\text{UNi}_{0.40}\text{Co}_{0.60}\text{Si}_2$: $\gamma^* = 42(1)$ mJ/(molK²), $B = 50(1)$ mJ/(molK⁴) and $\Delta = 54(1)$ K.

As can be inferred from Fig. 9(b), in the $\Delta C(T)/T$ derived for $\text{UNi}_{0.02}\text{Co}_{0.98}\text{Si}_2$ there is no λ -shaped anomaly, and only a broad hump occurs in the vicinity of $T^* = 6$ K, i.e. near the temperature of the anomaly evidenced in the magnetization curve [compare Fig. 2(b)]. Consequently, this feature in the specific heat data might be interpreted as a result of short range magnetic ordering or spin-glass state formation.

Another interesting feature, well visible in the specific heat of $\text{UNi}_{0.02}\text{Co}_{0.98}\text{Si}_2$, is a broad maximum located at about 30 K [Fig. 9(b)]. Similar anomaly is present also in pure UCoSi_2 [Fig. 9(b)] and in Th-doped UCoSi_2 . Preliminary results obtained for the latter alloys (to be published elsewhere) show that the position of this anomaly is independent of Th-content, yet its magnitude scales with the dilution of the uranium sublattice. This finding clearly indicates a single-ion character of the hump, which probably results from splitting the the $5f$ multiplet in crystalline-electric-field potential. Closer look at the $\Delta(C)/T$ data allows to recognize some faint features at 30 K also in UNiSi_2 and $\text{UNi}_{0.40}\text{Co}_{0.60}\text{Si}_2$ [Fig. 9(b)], being in line with the latter hypothesis. However, the Schottky contribution is here largely obscured by the magnetic contribution due to the ferromagnetic ordering.

Figure 9(c) displays the temperature dependencies of the increase in the magnetic entropy ΔS , defined as:

$$\Delta S = \int_{T_{\min}}^T \frac{\Delta C(T)}{T} dT, \quad (5)$$

where T_{\min} is the lower temperature limit in our experiments. As seen, ΔS in $\text{UNi}_{1-x}\text{Co}_x\text{Si}_2$ increases with increasing temperature up to about 100 K and then saturates at about 9 J/(mol K). The latter value is close to $R \ln 3$ (where R is the universal gas constant), which is expected for a thermally populated triplet or pseudotriplet. Assuming that the system studied has a magnetic doublet as a ground state, the first excited level is a singlet, lying about 100 K above the ground level. Negligible increase of ΔS above 100 K suggests

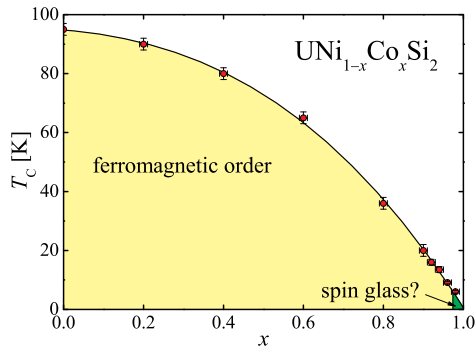


FIG. 10: (Color online) Tentative magnetic phase diagram of $\text{UNi}_{1-x}\text{Co}_x\text{Si}_2$. Solid line serves as a guide for the eye.

that the next excited CEF level (of unknown degeneracy) lies well above 300 K. Similar magnitude of CEF splitting is often observed in U-based systems.

The enlarged electronic contribution to the specific heat of UNiSi_2 and $\text{UNi}_{0.40}\text{Co}_{0.60}\text{Si}_2$ is a fingerprint of strong electronic correlations. Based on the value of the γ^* coefficient both materials can be qualified as moderately-enhanced Fermi liquids. Upon further increasing the Co-content the low-temperature heat capacity evolves into $C/T \sim -\ln T$ dependence, especially well resolved in UCoSi_2 , characteristic of non-Fermi liquid systems.

IV. SUMMARY

The presented experimental data revealed that the ferromagnetism and pronounced Kondo effect, observed in UNiSi_2 , is gradually suppressed upon stepwise substitution of Ni by Co. While in the $\text{UNi}_{1-x}\text{Co}_x\text{Si}_2$ alloys with $x < 0.98$ the phase transition exhibits clearly the ferromagnetic character, in the sample with $x = 0.98$ a spin-glass-like state with dominant spin fluctuations is seen. Whether any short-range order occurs in UCoSi_2 below 2 K, remains an open question.

Since the change of the unit cell volume of the system $\text{UNi}_{1-x}\text{Co}_x\text{Si}_2$ is relatively small and has different sign along the main crystallographic axes, the partial Ni/Co substitution cannot be treated as an approximation of hydrostatic pressure. Also the magnetic sublattice of uranium ions remains unaltered in the presented experiments. Therefore, the observed evolution of the physical properties of $\text{UNi}_{1-x}\text{Co}_x\text{Si}_2$ results most probably from electron

doping, because the electron configurations of nickel and cobalt differ from each other by one electron on the $3d$ shell.

Most interestingly, the extrapolation of the $T_C(x)$ curve to $x \rightarrow 1$ (Fig. 10) suggests the stoichiometric UCoSi_2 compound to be near the ferromagnetic quantum phase transition. Further experiments, performed at mK temperature range on single crystalline samples of UCoSi_2 , are needed to verify the latter hypothesis. In this context, particularly tempting seems a conjecture on the presence in UCoSi_2 of quantum critical point governed by ferromagnetic fluctuations and exclusion of the possibility of a rapid change of the character of the correlations in the alloys with $0.96 < x < 1$.

Acknowledgments

This work was supported by the Polish Ministry of Science and Higher Education within grant no. N N202 102338.

-
- ¹ G. R. Stewart, Rev. Mod. Phys. **73**, 797 (2001).
 - ² G. R. Stewart, Rev. Mod. Phys. **78**, 743 (2006).
 - ³ P. Coleman and A. J. Schofield, Nature **433**, 226 (2005).
 - ⁴ H. v. Löhneysen, A. Rosch, M. Vojta, and P. Wölfle, Rev. Mod. Phys. **79**, 1015 (2007).
 - ⁵ P. Gegenwart, Q. Si, and F. Steglich, Nature Physics **4**, 186 (2008).
 - ⁶ T. R. Kirkpatrick and D. Belitz, Phys. Rev. B **67**, 024419 (2003).
 - ⁷ M. Lenkewitz, S. Corsépius, G.-F. v. Blanckenhagen, and G. R. Stewart, Phys. Rev. B **55**, 6409 (1997).
 - ⁸ M. Nicklas, M. Brando, G. Knebel, F. Mayr, W. Trinkl, and A. Loidl, Phys. Rev. Lett. **82**, 4268 (1999).
 - ⁹ J.-P. Kappler, M. J. Besnus, P. Haen, and J. Sereni, Physica B **230–232**, 162 (1997).
 - ¹⁰ J. G. Sereni, T. Westerkamp, R. KÜchler, N. Caroca-Canales, P. Gegenwart, and C. Geibel, Phys. Rev. B **75**, 024432 (2007).
 - ¹¹ A. P. Pikul, N. Caroca-Canales, M. Deppe, P. Gegenwart, J. G. Sereni, C. Geibel, and F. Steglich, J. Phys.: Condens. Matter **18**, L535 (2006).

- ¹² T. Westerkamp, M. Deppe, R. Küchler, M. Brando, C. Geibel, P. Gegenwart, A. P. Pikul, and F. Steglich, *Phys. Rev. Lett.* **102**, 206404 (2009).
- ¹³ E. D. Bauer, V. S. Zapf, P.-C. Ho, N. P. Butch, E. J. Freeman, C. Sirvent, and M. B. Maple, *Phys. Rev. Lett.* **94**, 046401 (2005).
- ¹⁴ N. T. Huy, A. Gasparini, J. C. P. Klaasse, A. de Visser, S. Sakarya, and N. H. van Dijk, *Phys. Rev. B* **75**, 212405 (2007).
- ¹⁵ D. E. de Nijs, N. T. Huy, and A. D. Visser, *Phys. Rev. B* **77**, 140506 (2008).
- ¹⁶ S. S. Saxena, P. Agarwal, K. Ahilan, F. M. Grosche, R. K. W. Haselwimmer, M. J. Steiner, E. Pugh, I. R. Walker, S. R. Julian, P. Monthoux, et al., *Nature* **406**, 587 (2000).
- ¹⁷ D. Aoki, A. Huxley, E. Ressouche, D. Braithwaite, J. Flouquet, J.-P. Brison, E. Lhotel, and C. Paulsen, *Nature* **413**, 613 (2001).
- ¹⁸ N. T. Huy, A. Gasparini, D. E. de Nijs, Y. Huang, J. C. P. Klaasse, T. Gortenmulder, A. de Visser, A. Hamann, T. Görlach, and H. v. Löhneysen, *Phys. Rev. Lett.* **99**, 067006 (2007).
- ¹⁹ J. Larrea J., M. B. Fontes, A. D. Alvarenga, E. M. Baggio-Saitovitch, T. Burghardt, A. Eichler, and M. A. Continentino, *Phys. Rev. B* **72**, 035129 (2005).
- ²⁰ D. Kaczorowski, *Solid State Commun.* **99**, 949 (1996).
- ²¹ T. Taniguchi, H. Morimoto, Y. Miyako, and S. Ramakrishnan, *J. Magn. Magn. Mater.* **177–181**, 55 (1998).
- ²² A. Das, S. K. Paranjpe, P. Raj, A. Satyamoorthy, K. Shashikala, and S. K. Malik, *Solid State Commun.* **114**, 87 (2000).
- ²³ E. S. R. Gopal, *Specific Heats at Low Temperatures* (Plenum Press, New York, 1966).